RSC Advances

ROYAL SOCIETY OF CHEMISTRY

www.rsc.org/advances

Complicated synergistic effects between metal-π interaction and halogen bond involving MCCX

Meng Gao[1], Qingzhong Li[1,]*, Jianbo Cheng[1], Wenzuo Li[1], Hai-Bei Li[2,]*

[1] *The Laboratory of Theoretical and Computational Chemistry, School of Chemistry and Chemical Engineering, Yantai University, Yantai 264005, People's Republic of China*

[2] *School of Ocean, Shandong University, Weihai 264209, People's Republic of China*

*To whom all correspondence should be addressed:

 Dr. Qing-Zhong Li, E-mail: liqingzhong1990@sina.com

 Dr. Hai-Bei Li, E-mail: lihaibei@sdu.edu.cn

Abstract

The ternary systems FCCF⋯MCCX⋯NCH (M = Cu, Ag, Au, and Li; X = Cl, Br, and I) involving metal-π interaction and halogen bond have been studied by quantum chemical calculations at the MP2/aug-cc-pVTZ level of theory as well as the corresponding binary ones. The halogen substituent has a slight effect on the strength of metal-π interaction FCCF⋯MCCX, while the metal substitution has a prominent effect on the strength of halogen bond MCCX⋯NCH. In the ternary systems involving LiCCX, both Li-π interaction and halogen bond are simultaneously weakened compared to those in the dyads. Interestingly, the coinage-metal-π interaction and halogen bond are simultaneously strengthened in the ternary systems involving AgCCX. In the triads FCCF⋯CuCCX⋯NCH and FCCF⋯AuCCCl⋯NCH, the coinage-metal-π interaction is weakened but the halogen bond is strengthened. However, a reverse change is found for both interactions in the ternary systems involving AuCCBr and AuCCI. In general, due to the introduction of the second pertinent interaction, the halogen bond suffers a greater change in strength than the coinage-metal-π interaction.

Keywords: Halogen bonds; Coinage-metal-π interactions; Cooperative effects

1. Introduction

Non-covalent interactions, including hydrogen-,[1] halogen-,[2] pnicogen-,[3] chalcogen-,[4] and carbon-bonding,[5] are of great importance in chemistry and biology.[6-8] Essentially, these interactions are partly attributed to the charge transfer from the occupied orbitals of a Lewis base into the unoccupied orbitals of a Lewis acid.[9-12] Many studies have demonstrated that non-covalent interactions exhibit the synergistic effect,[13-15] which is a primary driving force for the formation of new materials and plays a critical role in providing the new functions of the complexes.

Analogously to hydrogen bonding in some respects,[16] halogen bonding (XB) has been exploited as a significant tool in crystal engineering,[17] supramolecular chemistry,[7,18,19] drug design,[20] and molecular recognition in biological systems.[21] Clark *et al.*[22] proposed the term "σ-hole" to describe the region with positive electrostatic potentials on halogen atom in RX (X = halogen). The shape of σ-hole depends on the symmetry of halogen-containing molecules and it would be asymmetric for the low symmetrical molecules.[23] σ-hole can interact with Lewis bases and thus gives rise to the formation of halogen bonding. Furthermore, this σ-hole accounts for the directionality of halogen bonding.[24] The strength of halogen bonding becomes stronger in the order of F $\ll$ Cl < Br < I,[25] although fluorine could also participate in halogen bonds particularly when it is adjoined with a strong electron-withdrawing group.[26] For example, F_2 forms a halogen-bonded complex with ammonia.[27] Legon has presented a review on the isomorphism of complexes B-F_2 (B = a Lewis base) and other dihalogen complexes.[10] Halogen bonding displays synergistic effects with itself and other types of non-covalent interactions.[28-31] For instance, the interaction of the pyridine with nitrogen coordinated to a transition metal center can provide an electron-withdrawing effect that increases the electrophilicity of the halogen substituent on the pyridine and, consequently, enhances its ability to form halogen bonding.[32,33]

The coordination of coinage metals (Cu, Ag, and Au) with alkenes or alkynes is also a kind of important non-covalent interaction, which plays important roles in heteroatom-hydrogen bond additions, cycloaddition chemistry, C_{sp}-H bond functionalizations, alkyne coupling and hydrogenations processes.[34,35] In these coinage metal adducts, according to the Dewar-Chatt-Duncanson (DCD) model,[36,37] electron density transfers from the π

orbitals of the hydrocarbon to the unfilled orbitals of the metal. At the same time, this interaction is reinforced by a reciprocal transfer of electrons from the *d*-orbitals of the metal into the π* anti-bonding orbitals of the hydrocarbon. However, the π-donation of alkyne→M dominates over the M→alkyne σ-back-donation.[38] Legon *et al*. have studied the complexes of C_2H_4···AgCl,[36] C_2H_2···AgCl,[37] and C_2H_4 or C_2H_2···CuCl[39] using rotational spectroscopy, and found that these complexes are isomorphic with the corresponding hydrogen-bonded series consisting of HX (X= Cl and Br)[40,41] and halogen-bonded series with XY (XY = ClF, Cl_2, BrCl, Br_2, and ICl).[42-44] The rotational spectrum of complex C_2H_2···AgCCH was further measured by microwave spectroscopy and studied with *ab initio* calculations.[45] The results showed that all complexes have a T-shaped structure with C_{2v} symmetry, and the coinage-metal-containing complexes are more strongly bound than hydrogen- or halogen-bonded species. Surprisingly, the fluorine substituents in acetylene strengthen the interaction between CuF and acetylene, due to the prominent deformation of the interacting subunits.[46]

Very recently, the new linear molecules Ag−C≡C−Cl and Cu−C≡C−Cl have been synthesized by a laser-ablation method and were unambiguously characterized by means of the rotational spectra.[47] Zhao and Feng[48] have performed quantum chemical calculations for halogen-bonded complexes MCCBr···NCH and HCCBr···NCM' (M, M' = Cu, Ag, and Au) at the MP2 level. They found that the transition metal atoms in the halogen donors result in a weakening of the halogen bonding, whereas those in the halogen acceptors lead to an enhancement of the halogen bondings.[48] Difluoroethyne FCCF has a linear geometry, the same with that of HCCH, but the quadrupole moment of the former (-0.6389 B) is much smaller than that of the latter (4.856 B),[49,50] being less (hyper)polarizable than other dihaloethynes.[50] In the present study, we paid our attention to the complexes FCCF···M−C≡C−X···NCH (M = Cu, Ag, and Au; X = Cl, Br, and I) involving both metal-π interaction and halogen bonding. We performed a theoretical study on the triads with the aim of investigating the mutual influence between metal-π interaction and halogen bond as well as the cooperativity effect between them. For comparison, the corresponding Li systems and some HCCH and $C_2(CN)_2$ counterparts have also been studied to understand the cooperativity between metal-π interaction and halogen bond.

2. Computational details

All complexes were optimized at the second-order Møller-Plesset perturbation theory (MP2) level with aug-cc-pVTZ basis set for all atoms except I, Cu, Ag, and Au atoms. For the coinage metal and I atoms, the aug-cc-pVTZ-PP basis set was adopted to account for relativistic effects. The frequency calculations were performed to confirm the optimized structures being the local minimum on the potential surfaces. Interaction energies were calculated using the supermolecular approach and corrected by the basis set superposition error (BSSE) using the counterpoise method.[51] All these calculations were performed with Gaussian 09 software.[52]

Natural orbital analysis (NBO) was carried out at the HF/aug-cc-pVTZ level via NBO 5.0 program.[53] GAMESS program[54] was used to perform the energy decomposition analysis for the interaction energy with the LMOEDA method[55] at the MP2/aug-cc-pVTZ level. The topological analysis of the electron density for all complexes was performed according to Bader's theory of atoms in molecules (AIM) at the MP2/aug-cc-pVDZ level by software AIM2000.[56] Molecular electrostatic potentials (MEPs) on the 0.001 electrons bohr^{-3} contour of the electronic density were calculated by using the Wavefunction Analysis–Surface Analysis Suite (WFA-SAS) program.[57]

3. Results and discussion

3.1. MEPs of MCCX

The MEP maps of M–C≡C–X (M = Li, Cu, Ag, and Au; X = Cl, Br, and I) are plotted in Fig. 1. It is evident from Fig. 1 that there are two positive MEP sites at both ends of molecule M–C≡C–X around X and M atoms. Thus, molecule M–C≡C–X could serve as a Lewis acid interacting with two Lewis bases at both ends of the molecule. Specially, both of X and M can respectively bind with Lewis bases FCCF and NCH to form a metal-π interaction and halogen bonding. The region of positive MEP on the metal atom is much larger than that on the halogen atom (Table 1 and Fig. 1), indicating that the metal atom is a stronger Lewis acid than the halogen atom. It is evident from Table 1 that the Cu of CuCCX has the biggest $V_{M,max}$ (most positive MEP on the metal atom), followed by the Au of AuCCX, and the $V_{M,max}$ on the Ag atom of AgCCX is the smallest. For the same coinage metal, the halogen substitution has little influence on the value of $V_{M,max}$ (Table 1). For example, for the molecule AuCCX (X =

Cl, Br, and I), $V_{Au,max}$ is around 0.15 a.u., *that is*, $V_{M,max}$ is independent on the halogen atom. On the contrary, the coinage metal substitution exhibits an obvious effect on the most positive MEP on the halogen atom ($V_{X,max}$). Taking MCCBr (M = Cu, Ag, Au) as an instance, $V_{Br,max}$ is 0.2510, 0.0229, and 0.0341 a.u. for CuCCBr, AgCCBr, and AuCCBr, respectively. Compared with $V_{X,max}$ (0.0347-0.0540 a.u.) in HCCX,[58] the metal substitution results in a decrease of $V_{X,max}$, and even the value of $V_{Cl,max}$ in LiCCCl is close to zero due to the strong electron-donating ability of Li atom. As expected, the value of $V_{X,max}$ shows an increasing tendency for the heavier halogen atom (Table 1).

3.2. Metal-π interaction and halogen bond

Fig. 2 shows the schemes of metal-π interaction and halogen bond binary interaction systems. It is evident from Fig. 2 that the FCCF molecule in the coinage metal complexes greatly deviates from the linear structure, while it has not such large deviation in the Li complexes. Thus, we calculated the interaction energies of coinage-metal-π interactions upon the basis of the geometries of FCCF in the complexes. The interaction energies and binding distances in these complexes are presented in Table 2. It is immediate that the coinage-metal-π interaction is much stronger than the halogen and lithium bonds, and the interaction energies of Cu- and Au-π interactions in the former case are even 15 times higher than that in the latter. Interestingly, for a given coinage metal, the strength of metal-π interaction is nearly the same in FCCF···MCCX (X = Cl, Br, and I) with the variation of the halogen atom. The strength of the metal-π interaction is in the order of Cu-π > Au-π > Ag-π, which is consistent with the value $V_{M,max}$ of MEPs on the coinage metals. As mentioned above, it is noteworthy that the Li-π interaction is much weaker than that of the coinage-metal-π interaction, although the positive MEP on the Li atom is greater than that on the coinage metal atom. We attribute this to the difference of electron structure between coinage metal and Li complexes, where the former has dual interactions of π-d* donation of alkyne→M and the d-π* back-donation of M→alkyne. As expected, the halogen bonding becomes stronger in the order of Cl < Br < I (Table 2), consistent with the positive MEP on the halogen atom. The electron-donating property of metal atom is responsible for the weak halogen bond with the interaction energy from -0.24 to -3.61 kcal/mol. For a given halogen atom, the coinage metal substituent weakens the halogen bond in the order of Au > Cu > Ag. Compared to Cu and Ag

substituents with nearly the same effect on the interaction energy of X···N halogen bonding, Au exhibits a little larger influence. Furthermore, the Li substitution brings out a prominent weakening effect on the halogen bond. All above results are supported by the change of most positive MEP on the halogen atom caused by the metal substituents (Table 1). Essentially, the strength of metal-π interaction depends on the nature of metal itself and has no bearing on the halogen substituents; however, the metal substituents have a large effect on the strength of halogen bonding.

We performed an AIM and NBO analyses for the metal-π interaction and halogen bond to get a deeper insight in the nature of both interactions. Seen in Fig. 2, a ring critical point (RCP) is found in the coinage-metal-π complexes, viewed as a new kind of metallocycle with significantly strong M–C linkages, while the Li-π complexes display a bond critical point (BCP). Similarly, a N···X BCP is observed in the halogen bond. In Table 3, we presented the results of the AIM analysis for the binary systems. The electron density between the coinage metal and the π system is significantly larger than that in the Li-π interaction and halogen bonding, although the type of critical point is different. This confirms the conclusion that the coinage-metal-π interaction is stronger than the lithium bond and halogen bond. Whether in the metal-π interaction or in the halogen bond, the Laplacian $\nabla^2\rho$ is positive, which reflects an excess of kinetic energy in bonds and a relative depletion of electronic charge along a bond path.[59] Generally, a positive energy density (*H*) corresponds to a purely closed-shell interaction, whereas a negative *H* value corresponds to bonds with any degree of covalent character.[59] Accordingly, the nature of the metal-π interaction prefers more covalent feature with a negative *H*, and the Li-π interaction is more ionic feature in nature with a positive *H* as well as the halogen bond.

The NBO analysis of the coinage metal-π complexes (see Table S1) shows a significant charge transfer from the π-system to the empty orbital of the coinage metal and a back-donation from the occupied *d* orbitals of the coinage metal into the π^*_{CC} anti-bonding orbital of the FCCF moiety. The donation contribution is more prominent than that from the back-donation. The donation contributions are mainly characterized by the orbital interaction of $\pi_{C\equiv C}\rightarrow\sigma^*_{C-M}$ in the Cu and Ag complexes but $\pi_{C\equiv C}\rightarrow Lp^*_M$ in the Au and Li complexes. It is not surprising that for the Li complexes, the back-donation vanishes and the donation also

reduces considerably due to the participated orbitals of Li being s and p different from the d orbitals in the coinage metal, so the interaction energy of lithium bonding is decreased significantly compared with that of the coinage-metal-π interaction. From Table S1, for the halogen bond, there is an orbital interaction between Lp_N and σ^*_{C-X} anti-bonding orbitals. Although the second-order perturbation energy is small in the range of $0.5 \sim 5.0$ kcal/mol, the variation for the each type of MCCX$\cdots$NCH with the same metal shows a consistency with the interaction energy of the complexes (Fig. S1).

To have a further insight into the nature of metal$\cdots\pi$ interaction and halogen bonding, the total interaction energy of the complexes was decomposed into five components: electrostatic energy (ES), exchange energy (EX), repulsion energy (REP), polarization energy (POL), and dispersion energy (DISP), collected in Table S2 and plotted in Fig. 3. In the coinage metal-π complexes, the value of each term is significantly greater than that in the other complexes. Based on the strong orbital interactions in the DCD model (Table S1), the coinage metal-π interaction possesses a large EX between the two molecular orbitals. Generally, the large EX is accompanied with a large REP due to the close contact between two monomers. In the complexes FCCF$\cdots$CuCCX and FCCF$\cdots$AgCCX (X = Cl, Br, and I), ES is a little more negative than POL. This indicates that both electrostatic and polarization interactions play an important role in the Cu-π and Ag-π interactions. On the contrary, the POL contribution is much larger ($\sim$30 kcal/mol) than that of ES in FCCF$\cdots$AuCCX complexes. The relatively large POL in the Au-π interaction suggests that the molecular orbitals undergo a significant change in their shapes. Among the five energy components from Table S2 and Fig. 3, it is evident that ES, EX, REP and POL contributions of Au-π interaction are larger than those of the Cu-π and Ag-π interactions, which is likely due to the higher electronegtivity of Au than Cu and Ag atoms. Interestingly, the POL term is dominant in the Li-π interaction. This is different from the lithium-bonded complex of $H_2CO\cdots LiF$,[60] with electrostatic interaction being dominant. The dominant POL contribution in the former is due to the T-shape structure of the Li-π complex, where Li atom directly point to the π orbitals leading to the large change in its shape. In the metal-π interaction, the variation of halogen substituent for a given coinage metal, the energy components and total energy are nearly the same with energy difference in 0.3 kcal/mol, *that is*, halogen substituents have little effect on the nature of the metal-π

8

interaction. On the other hand, in the X···N halogen-bonded complexes, the weak Cl···N halogen bonding is dominated by DISP. The DISP term has a comparable contribution to the Br···N halogen bond with ES. However, ES is dominant in the strongest I···N halogen bond.

3.3. Interplay between metal-π interaction and halogen bonding

Lu *et al*[33] found that the introduction of the second metal coordination force leads to the halogen bonding much stronger compared to that in the complexes of halogenated pyridine, where the nitrogen and halogen atoms are respectively taken as the Lewis base and acid in the metal coordination and halogen bond interactions. As mentioned above, molecule MCCX could act as the double Lewis acid interacting with two Lewis bases in both metal-π and halogen bond interactions, respectively. Thus it is interesting to study the interplay between the metal-π and halogen bond interactions in the triads FCCF···MCCX···NCH (M = Li, Cu, Ag, and Au; X = Cl, Br, and I).

The variations of binding distances of metal-π and halogen bond interactions and the electron densities at the intermolecular BCPs in the triads with respect to those in the dyads are listed in Table S3. It is evident from Table S3 that the binding distances of both lithium bonding and halogen bonding in FCCF···LiCCX···NCH system become longer in the triads than those in the dyads, respectively. This indicates that both lithium bonding and halogen bonding are weakened in the triads, which could be further evidenced by the reduction of electron densities at the π···Li and X···N BCPs in the triads (Table S3). The weakening of the interaction in the triads demonstrates that there is a negative synergistic effect between FCCF···LiCCX and LiCCX···NCH interactions. We explain this weakening by means of the electrostatic potentials and orbital interactions. The positive electrostatic potentials on the Li and X atoms are decreased in the dyads LiCCX···NCH and FCCF···LiCCX, respectively (Table S4). On the other hand, the orbital interactions of $\pi_{C\equiv C}\rightarrow Lp^*_{Li}$ in the lithium bonding and $Lp_N\rightarrow\sigma^*_{C-X}$ in the halogen bonding are slightly weakened (Table 4). Simultaneously, the occupancies on the bonding orbitals in both orbital interactions are decreased; on the contrary, those on the anti-bonding orbitials referring to both orbital interactions are increased. Furthermore, the changes in the occupancies on these orbitals are reduced in the triads with respect to the dyads, showing a consistent change with the perturbation energies of the orbital interactions. This consistency indicates that it is reliable to measure the change of interaction

strength based on the change of occupancy on the related orbitals.

Different from the features in FCCF···LiCCX···NCH system, the changes of binding distances in the triads consisting of coinage-metal-π and halogen bond interactions are complicated for the different coinage metal complexes. In the ternary systems involving CuCCX, the binding distance of the coinage-metal-π interaction is longer, while it becomes shorter for that of the halogen bond. Consistently, the electron density at the C···Cu BCP in the metal-π interaction decreases, where that at the N···X BCP in the halogen bonding increases. This indicates the coinage-metal-π interaction is weakened and the halogen bond is strengthened in the triads FCCF···CuCCX···NCH. Interestingly, for the ternary systems involving molecule AgCCX, the binding distances of FCCF···AgCCX and AgCCX···NCH become shorter as well as the electron densities at the corresponding BCPs increase, which demonstrates that both FCCF···AgCCX interaction and AgCCX···NCH halogen bonding are enhanced in the triads involving AgCCX due to the positive synergistic effect. It is evident from Table S3 that for FCCF···AuCCX···NCH, the strengths of FCCF···AuCCX and AuCCX···NCH interactions are dependent on the halogen atom. The Cl substituent gives rise to the strengthening of halogen bonding and weakening of the metal-π interaction, however, the contrary for the Br and I substituents. Furthermore, upon the basis of the variation value of binding distance and electron density for FCCF···AuCCX, the halogen substituents have small effect on the strength of FCCF···AuCCX interaction. To gain an insight into the charge redistribution upon the formation of complexes, electron density difference (EDD) maps are depicted in Fig. S2. The red lines represent the concentration of charge density and the blue ones are the regions with reduced charge density. For the coinage metal-π complexes, a region (blue) of density depletion is found on the coinage metal atom, while an area (red) of density accumulation is found between the Au and π bond. These features of EDD are almost identical for the triads and dyads, thus the weaker halogen bond has a slight effect on the stronger coinage-metal-π interaction.

Considering the dominant role of electrostatic interaction in the halogen bonding, we compare the variation of the most positive MEP ($\Delta V_{X,max}$) on the halogen atom in the dyads FCCF···MCCX with respect to that in the monomers. The positive MEP on the halogen atom (Table S4) is increased in the dyads FCCF···MCCX (M = Cu, Ag, Au; X = Cl, Br, I) in the

order of FCCF···CuCCX > FCCF···AgCCX > FCCF···AuCCX. And with the same coinage metal atom, the different halogen substituent has similar value $\Delta V_{X,max}$. It is interesting that the increase of the positive MEP on the halogen atom in the dyads FCCF···MCCX is linearly related with the change of halogen bonding distance in the triads FCCF···MCCX···NCH (Fig. 4A). On the other hand, the change of halogen bonding strength in the triads is in accordance with the variation of the strength of orbital interaction. It is evident from the second-order perturbation energy of $Lp_N \rightarrow \sigma^*_{C-X}$ orbital interaction in Table S5 that $Lp_N \rightarrow \sigma^*_{C-X}$ interaction becomes stronger in the triads FCCF···MCCX···NCH (M = Cu and Ag) and FCCF···AuCCCl···NCH, but is weaker in the triads FCCF···AuCCBr···NCH and FCCF···AuCCI···NCH than that in the dyads, which is in agreement with the change of halogen bonding strength (Table S3).

For the metal-π interaction in the triads, its change of binding distance shows a complicated relation with the variation of the $V_{M,max}$ on the metal atom (Fig. 4B), which is decreased in the dyads MCCX···NCH relative to that in the monomer MCCX (Table S4). With the decrease of $V_{M,max}$, the metal···π distance is almost not changed in the AuCCX complexes, longer in the CuCCX complexes and shorter in the AgCCX complexes. In the last complexes, no linear relationship is found between the shortening of Ag···π distance and $\Delta V_{Cu,max}$. This means that electrostatic interaction is not the sole primary determinant in the strength of coinage-metal-π interaction. According to the DCD model in the metal-π interaction, the C≡C bonding and anti-bonding orbitals in FCCF act as the donor orbital in the π-donation interaction and the acceptor orbital in the σ-back-donation interaction, respectively. These orbital interactions can be characterized with the change of occupancies (Δn) in the corresponding orbitals. Upon the complexation, the Δn in the C≡C bonding orbital is decreased and that in the C≡C anti-bonding orbital is increased (Table 5). The change of occupancies in both orbitals is consistent with the nature of the $\pi_{C≡C}$ donor orbital and the $\pi^*_{C≡C}$ acceptor orbital in the coinage-metal-π interaction. This provides the evidence for the existence of both orbital interactions in the coinage-metal-π interaction. Moreover, the change of occupancies in both orbitals is larger in the order of Ag < Cu < Au, consistent with the strength of the π···M interaction in FCCF···MCCX complex. However, a further analysis shows that the magnitude of $\Delta n_{C≡C}$ in triads is similar with that in dyads, indicating that the

11

π···M interaction in the triads has similar strength with that in the dyads based on the fact that the π-donation interaction is dominant in the coinage-metal-π interaction.

To have a better understanding for the variation of the coinage-metal-π interaction in the triads, the corresponding complexes of HCCH and NCCCCN are also studied. One can see in Table S6 that the π-lithium bond becomes stronger in the order of NCCCCN < FCCF < HCCH. It is known that there is no deformation for the π molecule in the lithium-bonded complexes and no σ-back-donation interaction is found in the lithium bond. Accordingly, the variation of π-lithium bond strength is dependent on the electron-withdrawing ability of substituents (H, F, and CN), which shows a consistent change with the strength of π-lithium bond. However, the strength of coinage-metal-π interaction is increased in the order of NCCCCN < HCCH < FCCF. This order has some difference from that of electron-withdrawing ability of substituents (H, F, and CN). Considering the fact that there are both π-donation interaction and σ-back-donation interaction in the coinage-metal-π interaction and the deformation of π molecule has great contribution to the stability of coinage-metal-π complexes,[46] we think that the stability of coinage-metal-π complexes is determined with a combination of the electron-withdrawing ability of substituent and the deformation of the π molecule. It is expected that the π-donation interaction is largest in the HCCH complexes and smallest in the NCCCCN complexes due to the strongest electron-withdrawing ability of CN, while the σ-back-donation interaction has a reverse result. The deformation of the π molecule can be estimated with the angle C≡C-Y (Y = H, F, and CN). Namely, the smaller angle C≡C-Y means a bigger deformation of the π molecule. It is found from Table S7 that the angle C≡C-Y becomes smaller in the order of HCCH > NCCCCN > FCCF. Consequently, the deformation of the π molecule is largest in the FCCF complexes and smallest in the HCCH complexes. Upon the trimerization, the angle C≡C-Y is nearly equal to that in the corresponding dyads (Table S7). In other words, the strength of coinage metal-π interaction is slightly changed in the triads.

3.4. Experimental evidences

To understand the significance of this work, experimental evidences for the coexistence of the coinage-metal-π interaction and halogen bonding in crystal materials are searched in the Cambridge Structural Database (CSD).[61] Only crystal structures with no disorder and

12

errors and R factors of less than 0.1 were considered. Figure 5 shows several crystal structures simultaneously with the coinage-metal-π and halogen bonding interactions, including ZUBNOZ, CIMXEC, CIMXAY, CESQOG, CUQLEG, RIZYIJ. In ZUBNOZ, the F$\cdots$F distance of 2.835 Å is shorter than the sum of their Van der Waals radius (2.94 Å), indicating the existence of halogen bonding. Simultaneously, Ag atom forms two metal-π interactions with 1,5-dimethyl-1,5-cyclooctadiene. In addition, the π systems in the metal-π interactions are also from ethene and benzene. A comparison of I$\cdots$O distance (3.445 Å and 3.404 Å) in CESQOG and the sum of their Van der Waals radius (3.50 Å) confirms the presence of halogen bonding. The model systems FCCF$\cdots$M$-$C$\equiv$C$-$X$\cdots$NCH are simpler than the above structures, but the conclusions obtained from this model are helpful to construct crystal materials with both types of interactions using experimental methods.

4. Conclusions

The linear molecule MCCX can form both a halogen bond with NCH when the halogen atom serves as a Lewis acid and a metal-π interaction with FCCF when the metal atom acts as a Lewis acid. According to the DCD model, there are three strong orbital interactions of $\pi_{C\equiv C}$ $\rightarrow$Lp$^*_M$, $\pi_{C\equiv C}$ $\rightarrow\sigma^*_{C-M}$, and Lp$_M$ $\rightarrow\pi^*_{C\equiv C}$ in the coinage metal-π interaction. However, there is only $\pi_{C\equiv C}\rightarrow$Lp$^*_M$ orbital interaction in the Li-containing complexes. The strength of coinage metal-π interaction in FCCF$\cdots$MCCX is related to the nature of the coinage metal and is stronger in the order of Ag$\cdots\pi <$ Au$\cdots\pi <$ Cu$\cdots\pi$. The halogen substituent has no effect on the strength of metal-π interaction. The strength of halogen bond in MCCX$\cdots$NCH mainly depends on the nature of the halogen atom. The metal substituent, particularly Li, weakens the halogen bond. In FCCF$\cdots$MCCX$\cdots$NCH, the halogen bond and metal$\cdots\pi$ interactions have complicated cooperative effects. Both interactions are enhanced in FCCF$\cdots$AgCCX$\cdots$NCH but weakened in FCCF$\cdots$LiCCX$\cdots$NCH. The halogen bond is strengthened and the metal-π interaction is attenuated in FCCF$\cdots$CuCCX$\cdots$NCH and FCCF$\cdots$AuCCCl$\cdots$NCH. Different with these in the latter complex, both interactions show a reverse change in FCCF$\cdots$AuCCBr$\cdots$NCH and FCCF$\cdots$AuCCI$\cdots$NCH. Generally, the strength of coinage-metal-π interaction has a slight change in the ternary complexes compared to the corresponding binary complexes. A search for crystal structures provides an evidence for the coexistence of both metal-π interaction and halogen bond, and the ternary complexes in our

study could be observed and characterized spectroscopically in supersonically expanded gas mixtures in the future.

Acknowledgements

Reference

1 G. A. Jeffref, New York: Oxford University Press, 1997.

2 A. C. Legon, *Phys. Chem. Chem. Phys.*, 2010, **12**, 7736–7747.

3 S. Zahn, R. Frank, E. Hey-Hawkins and B. Kirchner, *Chem. Eur. J.*, 2011, **17**, 6034–6038.

4 W. Z. Wang, B. M. Ji and Y. Zhang, *J. Phys. Chem. A*, 2009, **113**, 8132–8135.

5 S. J. Grabowski, *Phys. Chem. Chem. Phys.*, 2014, **16**, 1824–1834.

6 C. L. Perrin and J. B. Nielson, *Annu. Rev. Phys. Chem.*, 1997, **48**, 511–544.

7 A. R. Voth, F. A. Hays and P. S. Ho, *Proc. Natl. Acad. Sci. U. S. A.*, 2007, **104**, 6188–6193.

8 S. Scheiner, *Acc. Chem. Res.*, 2013, **46**, 280–288.

9 M. Yáñnez, P. Sanz. O. Mó, I. Alkorta, J. Elguro, *J. Chem. Theory Comput.*, 2009, **5**, 2763–2771.

10 A. C. Legon, *Angew. Chem. Int. Ed.*, 1999, **38**, 2686–2714.

11 L. Y. Guan and Y. R. Mo, *J. Phys. Chem. A*, 2014, **118**, 8911–8921.

12 A. Bauzá, T. J. Mooibroek and A. Frontera, *Angew. Chem. Int. Ed.*, 2013, **52**, 12317–12321.

13 J. H. Lee, J. Park, M. S. Lah, J. Chin and J. I. Hong, *Org. Lett.*, 2007, **9**, 3729–3731.

14 I. Alkorta, G. Sánchez-Sanz, J. Elguero and J. E. Del Bene, *J. Chem. Theory Comput.*, 2012, **8**, 2320–2327.

15 O. Mó, M. Yáñez, I. Alkorta and J. Elguero, *J. Chem. Theory Comput.*, 2012, **8**, 2293–2300.

16 P. Metrangolo, H. Neukirch, T. Pilati and G. Resnati, *Acc. Chem. Res.* 2005, **38**, 386–395.

17 P. Metrangolo, G. Resnati, T. Pilati and S. Biella, *Struct. Bond.*, 2008, **126**, 105–136.

18 P. Metrangolo, F. Meyer, T. Pilati, G. Resnati and G. Terraneo, *Angew. Chem. Int. Ed.*, 2008, **47**, 6114–6127.

19 H. M. Yamamoto, Y. Kosaka, R. Maeda, J. Yamaura, A. Nakao, T. Nakamura and R. Kato,

ACS Nano, 2008, **2**, 143–155.

20 Y. X. Lu, Y. T. Liu, Z. J. Xu, H. Y. Li, H. L. Liu and W. L. Zhu, *Expert Opin. Drug Discovery*, 2012, **7**, 375–383.

21 P. Auffinger, F. A. Hays, E. Westhof and P. S. Ho, *Proc. Natl. Acad. Sci. U. S. A.*, 2004, **101**, 16789–16794.

22 T. Clark, M. Hennemann, J. S. Murray and P. Politzer, *J. Mol. Model.*, 2007, **13**, 291–296.

23 M. H. Kolář, P. Carloni and P. Hobza, *Phys. Chem. Chem. Phys.*, 2014, **16**, 19111–19114.

24 P. Politzer, J. S. Murray and Timothy Clark, *Phys. Chem. Chem. Phys.*, 2010, **12**, 7748–7757.

25 P. Politzer, P. Lane, M. C. Concha, Y. G. Ma and J. S. Murray, *J. Mol. Model.*, 2007, **13**, 305–311.

26 P. Metrangolo, J. S. Murray, T. Pilati, P. Politzer, G. Resnati and G. Terraneo, *Cryst. Growth Des.*, 2011, **11**, 4238–4246.

27 H. I. Bloemink, K. Hinds, J. H. Holloway and A. C. Legon, *Chem. Phys. Lett.*, 1995, **245**, 598–604.

28 S. J. Grabowski and E. Bilewicz, *Chem. Phys. Lett.*, 2006, **427**, 51–55.

29 Q. Z. Li, Q. Q. Lin, W. Z. Li, J. B. Cheng, B. A. Gong and J. Z. Sun, *ChemPhysChem*, 2008, **9**, 2265–2269.

30 C. Estarellas, A. Frontera, D. Quiñonero and P. M. Deyà, *ChemPhysChem*, 2011, **12**, 2742–2750.

31 Y. X. Lu, Y. T. Liu, H. Y. Li, X. Zhu, H. L. Liu and W. L. Zhu, *J. Phys. Chem. A*, 2012, **116**, 2591–2597.

32 L. Brammer, G. M. Espallargas, and S. Libri, *CrystEngComm*, 2008, **10**, 1712–1727.

33 Y. H. Wang, W. H. Wu, Y. T. Liu, Y. X. Lu, *Chem. Phys. Lett.*, 2013, **578**, 38–42.

34 A. S. K. Hashmi, *Chem. Rev.*, 2007, **107**, 3180–3211.

35 A. Arcadi, *Chem. Rev.*, 2008, **108**, 3266–3325.

36 S. L. Stephens, D. P. Tew, V. A. Mikhailov, N. R. Walker and A. C. Legon, *J. Chem. Phys.*, 2011, **135**, 024315.

37 S. L. Stephens, W. Mizukami, D. P. Tew, N. R. Walker and A. C. Legon, *J. Chem. Phys.*, 2012, **137**, 174302.

38 H. V. R. Dias. J. A. Flores, J. Wu and P. Kroll, *J. Am. Chem. Soc.* 2009, **131**, 11249–11255.

39 S. L. Stephens, D. M. Bittner, V. A. Mikhailov, W. Mizukami, D. P. Tew, N. R. Walker and A. C. Legon, *Inorg. Chem.* 2014, **53**, 10722–10730.

40 P. D. Aldrich, A. C. Legon and W. H. Flygare, *J. Chem. Phys.*, 1981, **75**, 2126–2134.

41 A. C. Legon, P. D. Aldrich and W. H. Flygare, *J. Chem. Phys.*, 1981, **75**, 625–630.

42 J. M. A. Thumwood and A.C. Legon, *Chem. Phys. Lett.*, 1999, **310**, 88-96.

43 A. C. Legon, *Chem. Phys. Lett.*, 1999, **314**, 472–480.

44 A.C. Legon, *Struct. Bond.*, 2008, **126**, 17–64.

45 S. L. Stephens, D. P. Zalesk, W. Mizukami, D. P. Tew, N. R. Walker and A. C. Legon, *J. Chem. Phys.*, 2014, **140**, 124310.

46 G. Sánchez-Sanz, I. Alkorta, J. Elguero, M. Yáñez and O. Mó, *Phys. Chem. Chem. Phys.*, 2012, **14**, 11468–11477.

47 D. P. Zaleski, D. P. Tew, N. R. Walker and A. C. Legon. *J. Phys. Chem. A*, 2015, **119**, 2919−2925.

48 Q. Zhao and D. C. Feng, *J. Mol. Model.*, 2013, **19**, 1267–1271.

49 D. J. Gearhart, J. F. Harrison and K. L. C. Hunt, *Int. J. Quantum Chem.*, 2003, **95**, 697–705.

50 G. Maroulis and D. Xenides, *Int. J. Mol. Sci.*, 2003, **4**, 263–271.

51 S. F. Boys and F. Bernardi, *Mol. Phys.*, 1970**, 19**, 553−556.

52 M. J. Frisch, G. W. Trucks, H. B. Schlegel, G. E. Scuseria, M. A. Robb, J. R. Cheeseman, G. Scalmani, V. Barone, B. Mennucci, G. A. Petersson, H. Nakatsuji, M. Caricato, X. Li, H. P. Hratchian, A. F. Izmaylov, J. Bloino, G. Zheng, J. L. Sonnenberg, M. Hada, M. Ehara, K. Toyota, R. Fukuda, J. Hasegawa, M. Ishida, T. Nakajima, Y. Honda, O. Kitao, H. Nakai, T. Vreven, J. J. A. Montgomery, J. E. Peralta, F. Ogliaro, M. Bearpark, J. J. Heyd, E. Brothers, K. N. Kudin, V. N. Staroverov, R. Kobayashi, J. Normand, K. Raghavachari, A. Rendell, J. C. Burant, S. S. Iyengar, J. Tomasi, M. Cossi, N. Rega, J. M. Millam, M. Klene, J. E. Knox, J. B. Cross, V. Bakken, C. Adamo, J. Jaramillo, R. Gomperts, R. E. Stratmann, O. A. Yazyev, J. Austin, R. Cammi, C. Pomelli, J. W. Ochterski, R. L. Martin, K. Morokuma, V. G. Zakrzewski, G. A. Voth, P. Salvador, J. J. Dannenberg, S. A. Dapprich, D. Daniels, O. Farkas, J. B. Foresman, J. V. Ortiz, J.

Cioslowski and D. J. Fox, *Gaussian 09, Revision A.02*, Gaussian, Inc., Wallingford, CT, 2009.

53 A. E. Reed, L. A. Curtiss and F. Weinhold, *Chem. Rev.*, 1988, **88**, 899–926.

54 M. W. Schmidt, K. K. Baldridge, J. A. Boatz, S. T. Elbert, M. S. Gordon, J. H. Jensen, S. Koseki, N. Matsunaga, K. A. Nguyen, S. J. Su, T. L. Windus, M. Dupuis and J. A. Montgomery, *J. Comput. Chem.*, 1993, **14**, 1347–1363.

55 P. F. Su and H. Li, *J. Chem. Phys.*, 2009, **13**, 014102.

56 R. F. W. Bader, *AIM2000 Program*, McMaster University, Hamilton, Canada, 2000.

57 F. A. Bulat, A. Toro-Labbé, T. Brinck, J. S. Murray and P. Politzer, *J. Mol. Model.*, 2010, **16**, 1679–1691.

58 W .K. Tian and Q. Z. Li, *Int. J. Quantum Chem.*, 2015, **115**, 99–105.

59 W. D. Arnold and E. Oldfield, *J. Am. Chem. Soc.*, 2000, **122**, 12835–12841.

60 S. S. C. Ammal and P. Venuvanalingam, *J. Phys. Chem. A*, 2000, **104**, 10859–10867.

61 F. H. Allen, *Acta. Crystallogr. B*, 2002, **58**, 380–388.

Table 1 The most positive MEP on the halogen atom ($V_{X,max}$, a.u.) and the metal atom ($V_{M,max}$, a.u.) in the monomer MCCX (M = Li, Cu, Ag, and Au; X = Cl, Br, and I)

	$V_{X,max}$	$V_{M,max}$
CuCCCl	0.0168	0.1728
CuCCBr	0.0251	0.1732
CuCCI	0.0367	0.1732
AgCCCl	0.0145	0.1279
AgCCBr	0.0229	0.1285
AgCCI	0.0343	0.1286
AuCCCl	0.0257	0.1521
AuCCBr	0.0341	0.1519
AuCCI	0.0458	0.1508
LiCCCl	0.0010	0.3190
LiCCBr	0.0094	0.3203
LiCCI	0.0208	0.3216

Table 2 Binding distance (R, Å) and interaction energy (ΔE, kcal/mol) in the dyads

dyads	ΔE^{a}	R^{b}	dyads	ΔE	R^{b}
FCCF⋯CuCCCl	-47.51(-61.71)	1.786	CuCCCl⋯NCH	-1.18	3.104
FCCF⋯CuCCBr	-47.35(-61.56)	1.786	CuCCBr⋯NCH	-1.89	3.054
FCCF⋯CuCCI	-47.21(-61.46)	1.785	CuCCI⋯NCH	-2.93	3.053
FCCF⋯AgCCCl	-25.15(-34.83)	2.001	AgCCCl⋯NCH	-1.03	3.110
FCCF⋯AgCCBr	-25.15(-34.71)	2.002	AgCCBr⋯NCH	-1.82	3.060
FCCF⋯AgCCI	-24.99(-34.61)	2.002	AgCCI⋯NCH	-2.76	3.056
FCCF⋯AuCCCl	-45.64(-59.47)	1.962	AuCCCl⋯NCH	-1.69	3.057
FCCF⋯AuCCBr	-45.44(-59.21)	1.962	AuCCBr⋯NCH	-2.48	3.010
FCCF⋯AuCCI	-45.14(-58.93)	1.963	AuCCI⋯NCH	-3.61	3.009
FCCF⋯LiCCCl	-3.14	2.492	LiCCCl⋯NCH	-0.24	3.196
FCCF⋯LiCCBr	-3.17	2.486	LiCCBr⋯NCH	-0.85	3.129
FCCF⋯LiCCI	-3.20	2.485	LiCCI⋯NCH	-1.74	3.125

[a] Data in parentheses are the interaction energies obtained with the geometries of monomers frozen in the complexes.

[b] R is the distance between the central point of C≡C and the M in the metal-π interaction and the distance between the halogen atom and the N atom in the halogen bond.

Table 3 Electron density (ρ, au), Laplacian ($\nabla^2\rho$, au), and energy density (*H*, au) at the intermolecular critical point in the dyads[a]

dyads	ρ	$\nabla^2\rho$	*H*	dyads	ρ	$\nabla^2\rho$	*H*
FCCF···CuCCCl	0.125	0.324	-0.057	CuCCCl···NCH	0.009	0.033	0.001
FCCF···CuCCBr	0.125	0.324	-0.057	CuCCBr···NCH	0.011	0.042	0.002
FCCF···CuCCI	0.125	0.324	-0.057	CuCCI···NCH	0.014	0.048	0.001
FCCF···AgCCCl	0.105	0.349	-0.036	AgCCCl···NCH	0.009	0.033	0.001
FCCF···AgCCBr	0.104	0.349	-0.036	AgCCBr···NCH	0.011	0.041	0.002
FCCF···AgCCI	0.104	0.349	-0.036	AgCCI···NCH	0.014	0.048	0.001
FCCF···AuCCCl	0.125	0.358	-0.062	AuCCCl···NCH	0.010	0.037	0.002
FCCF···AuCCBr	0.125	0.358	-0.062	AuCCBr···NCH	0.012	0.045	0.002
FCCF···AuCCI	0.125	0.358	-0.062	AuCCI···NCH	0.016	0.052	0.001
FCCF···LiCCCl	0.009	0.049	0.003	LiCCCl···NCH	0.007	0.027	0.001
FCCF···LiCCBr	0.010	0.050	0.003	LiCCBr···NCH	0.010	0.036	0.001
FCCF···LiCCI	0.010	0.050	0.003	LiCCI···NCH	0.013	0.042	0.001

[a] Topological parameters correspond to the ring critical point (RCP) in the coinage metal-π interaction and the bond critical point (BCP) in the Li-π interaction and halogen bond.

Table 4 Second-order perturbation energies of the orbital interactions $Lp_N \rightarrow \sigma^*_{C-X}$ in the halogen bond (E^2_{XB}, kcal/mol) and $\pi_{C\equiv C} \rightarrow Lp^*_{Li}$ in the lithium bond (E^2_{LB}, kcal/mol) in the triads as well as their changes (ΔE^2, kcal/mol) relative to the dyads, change of occupancy (Δn, e) on the orbitals in the triads compared to the monomers

	FCCF···LiCCCl···NCH	FCCF···LiCCBr···NCH	FCCF···LiCCI···NCH
E^2_{XB}	0.62	1.69	3.20
ΔE^2_{XB}	-0.03	-0.08	-0.13
E^2_{LB}	10.28	10.40	10.45
ΔE^2_{LB}	-0.22	-0.26	-0.27
Δn_N	-0.0014(-0.0014)	-0.0035(-0.0036)	-0.0057(-0.0081)
Δn^*_{C-X}	0.0005(0.0005)	0.0021(0.0021)	0.0057(0.0057)
$\Delta n_{C\equiv C}$	-0.0198(-0.0201)	-0.0199(-0.0202)	-0.0198(-0.0201)
Δn^*_{Li}	0.0398(0.0408)	0.0399(0.0411)	0.0400(0.0415)

Note: Data in parentheses are from the respective dyads.

Table 5 Change of occupancy (Δn, e) on the orbitals for C≡C and *C≡C of the coinage-metal-π interaction in the dyads (D) and triads (T) relative to the monomers as well as their change ($\Delta\Delta n$, e) at the HF/aug-cc-pVTZ(PP) level

complexes	$\Delta n_{C\equiv C}(D)$	$\Delta n^*_{C\equiv C}(D)$	$\Delta n_{C\equiv C}(T)$	$\Delta n^*_{C\equiv C}(T)$	$\Delta\Delta n_{C\equiv C}$	$\Delta\Delta n^*_{C\equiv C}$
FCCF⋯CuCCCl⋯NCH	-0.1940	0.1966	-0.1933	0.2023	0.0007	0.0056
FCCF⋯CuCCBr⋯NCH	-0.1943	0.1960	-0.1934	0.2023	0.0009	0.0063
FCCF⋯CuCCI⋯NCH	-0.1942	0.1957	-0.1934	0.2037	0.0008	0.0080
FCCF⋯AgCCCl⋯NCH	-0.1585	0.1134	-0.1592	0.1191	-0.0007	0.0057
FCCF⋯AgCCBr⋯NCH	-0.1585	0.1127	-0.1592	0.1187	-0.0007	0.0060
FCCF⋯AgCCI⋯NCH	-0.1582	0.1122	-0.1588	0.1188	-0.0006	0.0066
FCCF⋯AuCCCl⋯NCH	-0.2560	0.2316	-0.2547	0.2377	0.0013	0.0061
FCCF⋯AuCCBr⋯NCH	-0.2557	0.2302	-0.2543	0.2374	0.0014	0.0072
FCCF⋯AuCCI⋯NCH	-0.2550	0.2297	-0.2533	0.2377	0.0017	0.0080

Figure captions

Fig. 1. MEP maps of MCCX (M = Li, Cu, Ag, and Au; X = Cl, Br, and I) with the most positive MEP (V_{max}). Color ranges, in a.u., are: red, greater than 0.03; yellow, between 0.03 and 0.02; green, between 0.02 and 0; and blue, less than 0.

Fig. 2. Schemes of FCCF⋯MCCX and MCCX⋯NCH (M = Li, Cu, Ag, and Au; X = Cl, Br, and I).

Fig. 3. Histogram for energy components.

Fig. 4. (A) The change of halogen bond (XB) distance ($\Delta R_{X\cdots N}$) in the triad relative to the corresponding dyad versus the change of the most positive MEP on the halogen atom ($\Delta V_{X,max}$) in the dyad FCCF⋯MCCX (M = Cu, Ag, Au, and Li) relative to the MCCX monomer. (B) The change of metal–π binding distance ($\Delta R_{metal-\pi}$) in the triad relative to the corresponding dyad versus the change of the most positive MEP on the metal atom ($\Delta V_{M,max}$) in the dyad MCCX⋯NCH relative to the MCCX monomer.

Fig. 5. Several crystal structures with metal-π and halogen bonding interactions. The unit of distance is angstrom.

Fig. 1

Fig. 2.

FCCF⋯MCCX   FCCF⋯LiCCX

MCCX⋯NCH

(M=Cu, Ag, Au; X=Cl, Br, I)

Fig. 3.

Fig. 4.

Fig. 5.

ZUBNOZ

CIMXEC

CUQLEG

CIMXAY

CESQOG

RIZYIJ
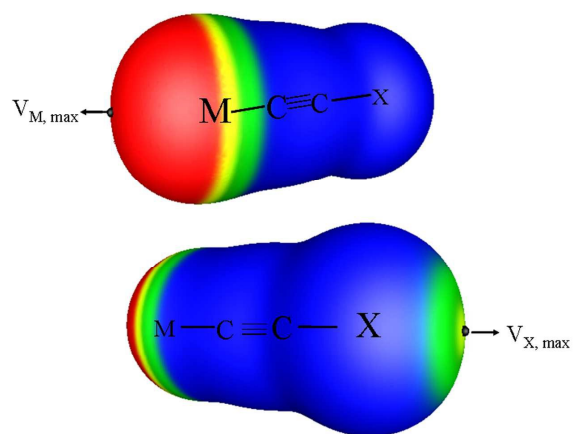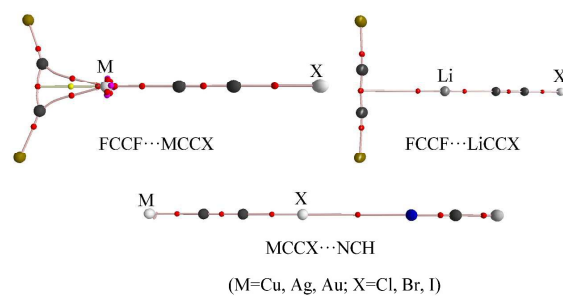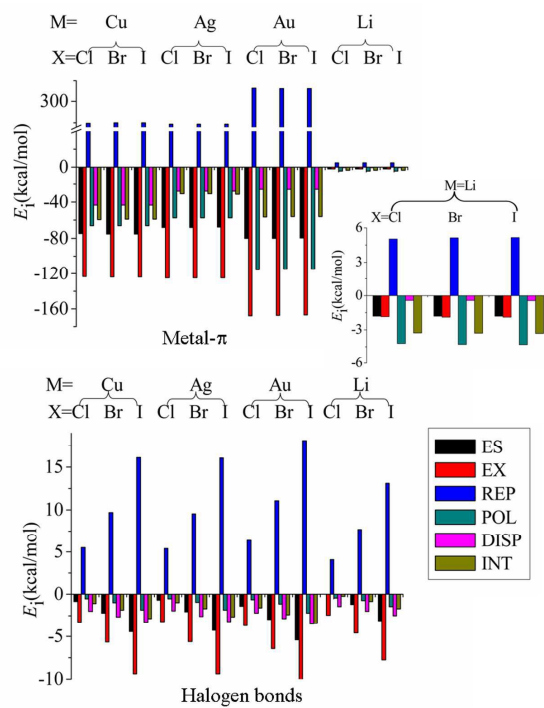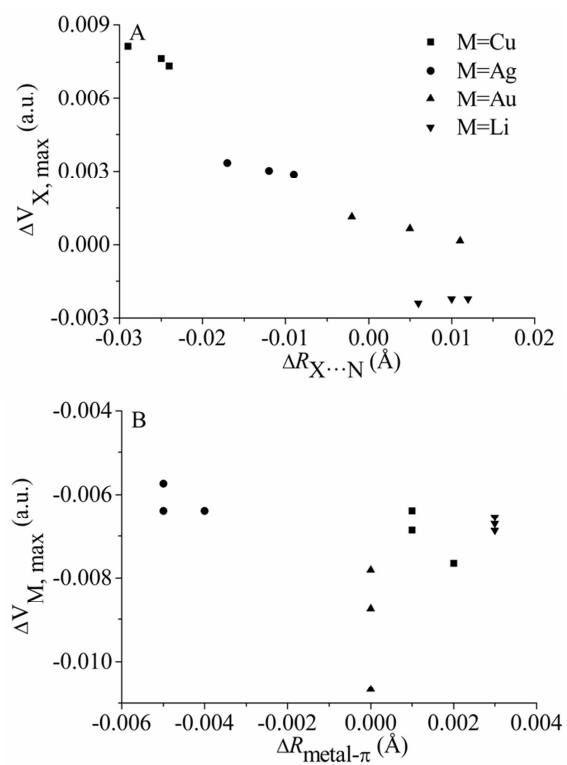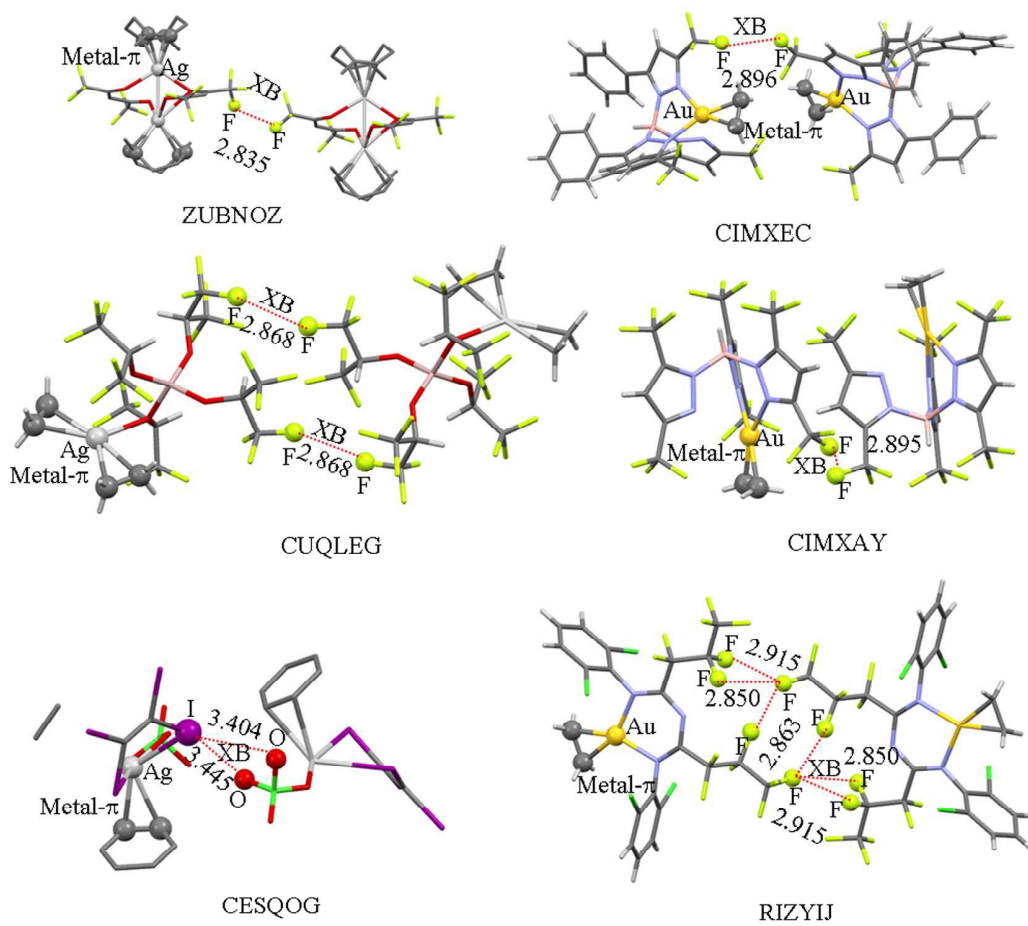
TOC
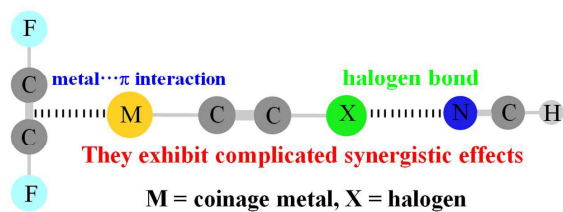
Complicated synergistic effects have been found between metal-π interaction and halogen bond in the complexes FCCF···MCCX···NCH (M = Li, Cu, Ag, and Au; X = Cl, Br, and I).